

Unusual Mobility of Cesium via a Reversible Topotactic Dehydration Reaction in a New Hydroxygallophosphate with an Intersecting Tunnel Structure

J. Lesage, A. Guesdon,* M. Hervieu, and B. Raveau

Laboratoire CRISMAT, UMR 6508 CNRS ENSICAEN, 6 Bd Maréchal Juin, 14050 Caen Cedex, France

Received February 3, 2006

The investigation of the system Cs–Ga–P–O by hydrothermal synthesis has allowed a new hydrated hydroxygallophosphate with an intersecting tunnel structure, $\text{Cs}_2\text{Ga}_6(\text{OH})_2(\text{PO}_4)_6 \cdot 1.55\text{H}_2\text{O}$, to be synthesized. It crystallizes with a monoclinic symmetry in the $P2_1/a$ space group with $a = 10.2190(4)$ Å, $b = 13.9565(15)$ Å, $c = 17.260(2)$ Å, and $\beta = 90.193(5)^\circ$ ($V = 2461.6(4)$ Å³, $Z = 4$). The detailed analysis of the structure shows that it consists of $[\text{Ga}_2(\text{OH})\text{P}_2\text{O}_{11}]_\infty$ layers interconnected through $[\text{GaPO}_6]_\infty$ chains forming the host lattice $[\text{Ga}_6(\text{OH})_2(\text{PO}_4)_6]_\infty$, built up of PO_4 and GaO_4 tetrahedra and $\text{GaO}_4(\text{OH})$ trigonal bipyramids. The structure presents a pseudo-orthorhombic symmetry, its monoclinic symmetry being imposed only by the configuration of the $[\text{GaPO}_6]_\infty$ chains and the positions of the Cs^+ cation and H_2O molecules sitting at the tunnels intersection. The electron microscopy and X-ray diffraction study versus temperature shows that this hydrated phase exhibits a topotactic dehydration toward $\text{Cs}_2\text{Ga}_6(\text{OH})_2(\text{PO}_4)_6$. The latter phase presents a $Pcab$ orthorhombic symmetry and its framework is isotypic to that of $(\text{CH}_3\text{NH}_3)_2\text{Ga}_6(\text{OH})_2(\text{PO}_4)_6$. A remarkable displacement of one of the Cs^+ cations, by about 3 Å, is observed during the dehydration. This reaction is reversible: placed in water, the dehydrated phase gives back the hydrated one.

Introduction

After the discovery of the microporous aluminophosphates by Wilson et al.,^{1,2} the systems “Al–P–O” and “Ga–P–O” were investigated by many authors, using hydrothermal synthesis with various amines as templating agents in order to produce opened frameworks with attractive catalytic properties. It was shown that the size and the shape of the amine molecule dictate the geometry of the framework of these compounds. In this respect, the cesium aluminophosphates and gallophosphates are of interest, due to the large size of the Cs^+ cation, intermediate between that of amines and smaller alkaline cations. Several anhydrous cesium aluminophosphates have been synthesized by solid-state reactions. It is the case of the triphosphates $\text{Cs}_2\text{MP}_3\text{O}_{10}$ ($M = \text{Al}, \text{Ga}$) with a layer structure^{3,4} and $\text{CsAl}_3(\text{P}_3\text{O}_{10})_2$,⁵ the tetrametaphosphate $\text{CsGa}(\text{PO}_3)_4$,⁶ and the pentaphosphate $\text{CsGa}_2\text{P}_5\text{O}_{16}$ ⁷ with a tunnel structure. Gallium hydroxyphosphates were also synthesized, but in aqueous solution. This is exemplified by the four forms of $\text{CsGaHP}_3\text{O}_{10}$ which are

all hydrogen triphosphates, three of them exhibiting a two-dimensional layer structure,^{8–10} whereas the fourth one consists of a 3D tunnel structure,¹¹ and by the hydrogen diphosphate $\text{Cs}_2\text{GaH}_3(\text{P}_2\text{O}_7)_2$,¹² which consists of a one-dimensional structure. In contrast to aluminophosphates templated with amines, it seems that very few cesium gallium phosphates or hydroxyphosphates, containing neutral molecules, like water, have been synthesized to date. Nevertheless, one interesting example is given by the cesium hydrogen gallophosphate $\text{Cs}_2\text{Ga}(\text{H}_2\text{PO}_4)(\text{HPO}_4)_2 \cdot \text{H}_3\text{PO}_4 \cdot 0.5\text{H}_2\text{O}$,¹³ whose structure consists of columns of corner-shared PO_4 tetrahedra and GaO_6 octahedra interconnected through Cs^+ cations and H_3PO_4 and H_2O molecules. The method of synthesis of the latter compound, using microwave heating of a mixture of different species in solutions of phosphoric acid, suggests that special conditions are required to introduce neutral molecules besides Cs^+ cations in the new framework. We have thus revisited the Cs–Ga–P–O system, using hydrothermal synthesis. We report herein on a cesium gallium hydroxyphosphate $\text{Cs}_2\text{Ga}_6(\text{OH})_2(\text{PO}_4)_6 \cdot x\text{H}_2\text{O}$ ($x \approx 1.55$), whose tunnel structure is closely related

* To whom correspondence should be addressed. E-mail: anne.guesdon@ensicaen.fr.

- (1) Wilson, T.; Lok, B. M.; Flanigen, E. M. U.S. Patent 4,310,440, 1982.
- (2) Wilson, T.; Lok, B. M.; Messina, C. A.; Cannan, T. R.; Flanigen, E. M. *J. Am. Chem. Soc.* **1982**, *104*, 1146.
- (3) Nandini Devi, R.; Vidyasagar, K. *J. Chem. Soc., Dalton Trans.* **2000**, 1605.
- (4) Guesdon, A.; Daguts, E.; Raveau, B. *J. Solid State Chem.* **2002**, *167*, 258.
- (5) Lesage, J.; Guesdon, A.; Raveau, B. *J. Solid State Chem.* **2005**, *178*, 1212.
- (6) Grunze, I.; Palkina, K. K.; Chudinova, N. N.; Guzeeva, L. S.; Avaliani, M. A.; Maksimova, S. I. *Izv. Akad. Nauk SSR, Noerg. Mater.* **1987**, *23*, 610.
- (7) Lesage, J.; Guesdon, A.; Raveau, B. *Solid State Sci.* **2004**, *6*, 697.

- (8) Chudinova, N. N.; Grunze, I.; Guzeeva, L. S.; Avaliani, M. A. *Inorg. Mater.* **1987**, *23*, 534.
- (9) Mi, J. X.; Borrmann, H.; Huang, Y. X.; Zhao, J. T.; Kneip, R. Z. *Kristallogr. NCS* **2003**, *218*, 169.
- (10) Anisimova, N.; Bork, M.; Hoppe, R.; Meisel, M. Z. *Anorg. Allg. Chem.* **1995**, *621*, 1069.
- (11) Mi, J. X.; Borrmann, H.; Huang, Y. X.; Zhao, J. T.; Kneip, R. Z. *Kristallogr.* **2003**, *218*, 167.
- (12) Grunze, I.; Maximova, S. I.; Palkina, K. K.; Chibiskova, N. T.; Chudinova, N. N. *Izv. Akad. Nauk SSR, Noerg. Mater.* **1988**, *24*, 264.
- (13) Anisimova, N.; Chudinova, N.; Hoppe, R.; Serafin, M. Z. *Anorg. Allg. Chem.* **1997**, *623*, 39.

to that of $(\text{CH}_3\text{NH}_3)_2\text{M}_6(\text{OH})_2(\text{PO}_4)_6$ with $\text{M} = \text{Al}, \text{Ga}$.^{14,15} We show that this novel tunnel structure can be dehydrated topotactically into a new hydroxyphosphate, $\text{Cs}_2\text{Ga}_6(\text{OH})_2(\text{PO}_4)_6$, which is isotopic to the methylammonium phase¹⁴ and that this reaction is reversible in the presence of water. Moreover, one observes an unusual mobility of a cesium cation which moves by about 3 Å, between two crystallographic sites during the hydration–dehydration reactions.

Chemical Synthesis of $\text{Cs}_2\text{Ga}_6(\text{OH})_2(\text{PO}_4)_6 \cdot x\text{H}_2\text{O}$ ($x \approx 1.55$)

The exploration of the Cs–Ga–P–O system in hydrothermal conditions was carried out from mixtures of CsOH (50% Alfa Aesar), Ga_2O_3 (Alfa Aesar 99.9%), and H_3PO_4 (85% Prolabo Rectapur). Single crystals of the novel phase $\text{Cs}_2\text{Ga}_6(\text{OH})_2(\text{PO}_4)_6 \cdot x\text{H}_2\text{O}$ ($x \approx 1.55$) were obtained for the Cs:Ga:P molar ratio corresponding to 1:2:2, added with 2 mL of water. For the synthesis, the above solution (pH \approx 1.5) was placed in a 21 mL Teflon-lined stainless steel Parr autoclave. It was heated at 180 °C for 48 h and then cooled to room temperature at 8 °C/h. The resulting product (pH \approx 6) was filtered off, washed with water, and dried in air. A white powder containing colorless crystals was obtained.

Many attempts, involving various conditions, were performed to synthesize a monophasic sample, but all of them failed. However, it was possible to synthesize crystals in a rather large amount using the following two-steps method. In the first step, $(\text{NH}_4)_2\text{HPO}_4$ (Prolabo Rectapur 99%) and Ga_2O_3 (in the molar proportion 1:1 for Ga:P) were finely ground in an agate mortar. This mixture was heated at 400 °C in air for 12 h in order to decompose $(\text{NH}_4)_2\text{HPO}_4$. In the second step, the resulting powder was finely ground again and placed in a 21 mL Teflon-lined autoclave with 5 mL of water and a 50% aqueous solution of cesium hydroxide, leading to a mixture containing Cs, Ga, and P in the 1:3:3 molar ratio. It was heated at 180 °C for 10 h and slowly cooled to 130 °C (2 °C/h). The resulting product was filtered off, washed with water, and dried in air, leading to a white powder containing rather large platy and stick-like colorless crystals as major phase. These crystals were manually sorted out in order to perform further studies, described below.

Determination of the Composition of $\text{Cs}_2\text{Ga}_6(\text{OH})_2(\text{PO}_4)_6 \cdot x\text{H}_2\text{O}$ ($x \approx 1.55$)

Semiquantitative analyses of some colorless crystals extracted from the preparations were first performed with an OXFORD 6650 microprobe mounted on a PHILIPS XL30 FEG scanning electron microscope. They revealed the presence of Cs, Ga, and P elements in the approximative 13:43:44 percentage in the crystals, in agreement with the cationic composition deduced from the single-crystal X-ray diffraction study (14:43:43).

Transmission electron microscopy (TEM) observations were also carried out with a JEOL 200 CX electron

microscope equipped with a Kevex EDS analyzer. For this purpose, single crystals of the new phase were crushed in alcohol and the small crystallites in suspension were deposited onto a holey carbon film supported by a copper grid. The EDS analysis confirms the cationic distribution homogeneity “ $\text{Cs}_2\text{Ga}_6\text{P}_6$ ”.

Bearing in mind the X-ray diffraction study (see above), the presence of water and hydroxyl groups was checked by thermogravimetry, using a TGA 92-16.18 Setaram microbalance. A preliminary investigation indicated that the compound contained physisorbed water. Thus, the following protocol was adopted: 15.43 mg of the powder sample was placed in a platinum crucible in air and heated in the microbalance at 100 °C, with a dwelling time of 5 h in order to remove all the physisorbed water. The sample was then heated at 1 °C/min up to 450 °C. After the expected loss of physisorbed water a two-step weight loss was clearly observed. The first step occurs just above 100 °C and extends up to about 350 °C, corresponding to a weight loss of 2.18%, equivalent to 1.59 H_2O mole per formula unit, in agreement with the structural study which evidences 1.55(2) H_2O in the structure. The second weight loss is observed above 400 °C and corresponds to a weight loss of 1.42%, in agreement with the departure of one water molecule issued from the two hydroxyl groups condensation (expected theoretical value 1.40%).

Single-Crystal X-ray Diffraction Study: Structure Determination of $\text{Cs}_2\text{Ga}_6(\text{OH})_2(\text{PO}_4)_6 \cdot x\text{H}_2\text{O}$ ($x \approx 1.55$)

Colorless single crystals of the new phase were studied with a BRUKER-NONIUS Kappa CCD four-circle diffractometer equipped with a bidimensional CCD detector and using Mo K α radiation. Data collections were made at 293 K, using the experimental conditions listed in Table 1. The cell parameters reported in Table 1 were accurately determined from the whole registered frames. Data were reduced and corrected for Lorentz and polarization effects with the EvalCCD package.¹⁶ Absorption corrections were calculated by the SADABS program.¹⁷ Structure determination and refinement was performed with the JANA2000 program.¹⁸

Two kinds of crystals were obtained for the new phase either as very thin lamellae perpendicular to the c axis or as hand stick-like crystals parallel to the a axis.

The examination of the images issued from the crystal test and the cell determined by the programs of the EVALCCD package¹⁶ revealed a pseudo-orthorhombic symmetry, with a β angle ranging from about 90.1° to 90.5°, whatever the shape of the studied crystal. These observations suggested the possible existence of a systematic pseudo-merohedral twin. The choice of the single-crystal registered for the structure determination and refinement consisted of finding a crystal large enough to have good diffraction data, with a β angle as far as possible from 90° to avoid a twinning ratio too close to 50%. A crystal with dimensions of 0.321×0.039

(14) Glasser, F. P.; Howie, R. H.; Kan, Q. *Acta Crystallogr., Sect. C* **1994**, 50, 848.

(15) Chippindale, A. M.; Powel, A. V.; Jones, R. H.; Thomas, J. M.; Cheetham, A. K.; Huo Q. H.; Xu, R. *Acta Crystallogr., Sect. C* **1994**, 50, 1537.

(16) Duisenberg, A. J. M.; Kroon-Batenburg, L. M. J.; Schreurs, A. M. *J. Appl. Crystallogr.* **2003**, 36, 220.

(17) Sheldrick, G.; Blessing, B. *Acta Crystallogr., Sect. A* **1995**, 51, 33.

(18) Petricek, V.; Dusek, M. *The crystallographic computing system JANA2000*; Institute of Physics: Praha, Czech Republic, 2000.

Table 1. Summary of Crystal Data, Intensity Measurements, and Structure Refinement Parameters for Cs₂Ga₆(OH)₂(PO₄)₆·xH₂O (x ≈ 1.55) and Cs₂Ga₆(OH)₂(PO₄)₆

	Cs ₂ Ga ₆ (OH) ₂ (PO ₄) ₆ ·xH ₂ O (x ≈ 1.55)	Cs ₂ Ga ₆ (OH) ₂ (PO ₄) ₆
crystal dimensions (mm)	0.321 × 0.039 × 0.034	0.337 × 0.063 × 0.046
space group	<i>P2₁/a</i>	<i>Pcab</i>
cell dimensions	<i>a</i> = 10.2190(4) Å <i>b</i> = 13.9565(15) Å <i>c</i> = 17.260(2) Å <i>β</i> = 90.193(5)°	<i>a</i> = 10.1662(4) Å <i>b</i> = 13.9762(12) Å <i>c</i> = 16.931(2) Å
Volume	2461.6(4) Å ³	2405.6(4) Å ³
Z	4	4
<i>ρ</i> calc	3.5471 g cm ⁻³	3.5550 g cm ⁻³
<i>λ</i> (Mo K α)	0.71069 Å	0.71069 Å
scan strategies	<i>φ</i> and <i>ω</i> scans 1.4°/frame 120 s/° 2 iterations Dx = 34 mm	<i>φ</i> and <i>ω</i> scans 0.5°/frame 100 s/° 2 iterations Dx = 34 mm
<i>θ</i> range for data collection	5.85° ≤ <i>θ</i> ≤ 37.50°	5.84° ≤ <i>θ</i> ≤ 40.00°
measured reflns	39034	46728
independent reflns	12372	7435
independent reflns with <i>I</i> > 3 σ	7681	5111
<i>μ</i> (mm ⁻¹)	9.899	10.121
parameters refined	398	195
agreement factors	<i>R</i> = 4.19%; <i>R_w</i> = 3.96%	<i>R</i> = 2.72%; <i>R_w</i> = 2.74%
weighting scheme	<i>w</i> = 1/($\sigma(F)^2 + 1 \times 10^{-4} F^2$)	<i>w</i> = 1/($\sigma(F)^2 + 1 \times 10^{-4} F^2$)
temp of measurement	293 K	293 K

× 0.034 mm³, i.e., a stick-like shape (along the *a* axis) and an intermediate *β* value of 90.193(5)°, was selected.

The *hkl* precession diagrams performed from the collected data clearly exhibited a macroscopic mosaicity, mainly around the *a** axis. The integration of the diffraction spots was thus performed with the introduction of an anisotropic mosaicity parameter.

The observed systematic absences *h0l*: *h* = 2*n* + 1 and *0k0*: *k* = 2*n* + 1 correspond to the centrosymmetric space group *P2₁/a* (No. 14). The structure was determined using the heavy atom method and successive difference Fourier synthesis and Fourier synthesis. In a first time, no twin law was introduced. The refinement of the atomic coordinates and the isotropic thermal parameters of all atoms led then to very high reliability factors (*R* = 0.1950 and *R_w* = 0.2526). In addition, the isotropic thermal parameter of the O(27) atom showed a negative value and it remained an important electronic density residue (17.89 e⁻/Å³) at 0.77 Å of O(28). It was also impossible to refine the anisotropic thermal parameters of any atom. Because of the probable existence of a pseudo-merohedral twin in our crystal, a second data collection was performed with a Dx of 90 mm, to determine the twin law and, more precisely, to choose between a mirror perpendicular to *a** or to *c** as the twinning element. The examination of the [*h0l*] reciprocal raws evidences that the splitting of the diffraction spots was not increasing with *l* but with *h*. The twinning element was thus identified as a mirror perpendicular to *c** and the corresponding matrix [1 0 0.004/0 1 0/0 0 -1] was introduced for the structure determination and refinement, which were performed using the first data collection (Dx = 34 mm). During the refinement, two *hkl* and *hk-l* spots were considered to be completely overlapped if their maximum angular difference did not exceed 0.25°. This value must be compared with the deviation of about 0.2° with respect to the orthorhombic symmetry, to take into account the supposed pseudo-

merohedry of the system. As a matter of fact, this refinement led to the reliability factors *R* = 0.0432 and *R_w* = 0.0409, with all atoms described by positive anisotropic ellipsoids. However, some residual electronic densities were observed close to Cs(1) (2.38 e⁻/Å³, located at 0.67 Å of Cs(1)): its anharmonic ADPs were thus refined (3rd order), leading to *R* = 0.0421 and *R_w* = 0.0398. The maximum residual electronic density was 1.47 e⁻/Å³.

The examination of bond valence sum (BVS) calculations¹⁹ led for the cationic elements (i.e., cesium, gallium, and phosphorus) to values close to the theoretical ones (i.e., 1, 3, and 5, respectively). Most of the oxygen anions present the expected value of 2, except O(5) and O(18) for which the BVS calculated values are 1.24 and 1.20, respectively, suggesting the presence of hydroxyl groups. Finally, O(27) and O(28) were identified as water molecules since they present BVS values of 0.21 and 0.25, respectively. The positions of the two hydrogen atoms linked to O28 (H(28a) and H(28b)) were determined and their isotropic displacement parameters were refined but constrained to adopt the same value. It was not possible to determine the atomic coordinates of the hydrogen atoms for the H₂O(27) water molecule, neither for the HO(5) and HO(18) hydroxyl groups. Note that the site hosting the water molecule O(27) is only partially occupied, with an occupancy rate refined to 0.549(19). The twin fraction was refined to 0.3285(7). The final atomic coordinates, equivalent isotropic displacement parameters, site occupancies, and their estimated standard deviations are listed in Table 2. They correspond to reliability factors *R* = 0.0419 and *R_w* = 0.0396. The distances and angles in the structure, as well as the BVS calculations, are reported in tables given as Supporting Information (S1a and S2a).

(19) Brese, N. E.; O'Keeffe, M. *Acta Crystallogr., Sect. B* **1991**, *47*, 192.

Table 2. Positional Parameters, Atomic Displacement Parameters, Site Occupancy, and Their Estimated Standard Deviations in $\text{Cs}_2\text{Ga}_6(\text{OH})_2(\text{PO}_4)_6 \cdot x\text{H}_2\text{O}$ ($x \approx 1.55$)^a

atom	<i>x</i>	<i>y</i>	<i>z</i>	U_{eq} (Å ²)	occupancy
Cs(1)	0.45294(9)	0.32130(7)	0.48291(5)	0.03639(15)	1
Cs(2)	0.70123(4)	0.30188(3)	-0.00271(2)	0.02239(10)	1
Ga(1)	0.16542(5)	0.51388(4)	0.19739(3)	0.00815(14)	1
Ga(2)	0.11788(6)	0.43536(4)	0.39560(3)	0.00816(14)	1
Ga(3)	0.38062(6)	0.75561(4)	0.30301(3)	0.00971(13)	1
Ga(4)	0.66794(5)	0.48331(4)	0.30275(3)	0.00802(13)	1
Ga(5)	0.62055(6)	0.56612(4)	0.10542(3)	0.00757(13)	1
Ga(6)	0.93267(5)	0.23943(4)	0.20020(3)	0.00948(14)	1
P(1)	0.37396(13)	0.53773(10)	0.34143(7)	0.0095(3)	1
P(2)	0.37531(13)	0.42964(10)	0.08273(7)	0.0075(3)	1
P(3)	0.13160(13)	0.74079(10)	0.19970(7)	0.0089(3)	1
P(4)	0.86522(13)	0.45444(10)	0.15991(7)	0.0086(3)	1
P(5)	0.87149(13)	0.57389(10)	0.41807(7)	0.0077(3)	1
P(6)	0.68656(12)	0.25124(10)	0.30022(7)	0.0093(3)	1
O(1)	-0.0012(4)	0.4953(3)	0.1401(2)	0.0157(11)	1
O(2)	0.3281(4)	0.5242(3)	0.2576(2)	0.0146(11)	1
O(3)	0.2400(4)	0.4417(3)	0.1192(2)	0.0139(10)	1
O(4)	0.1723(4)	0.6426(3)	0.1704(2)	0.0154(11)	1
O(5)	0.0839(3)	0.4773(3)	0.2884(2)	0.0131(10)	1
O(6)	0.1421(3)	0.3882(3)	0.5000(2)	0.0120(9)	1
O(7)	-0.0483(3)	0.4815(3)	0.4169(2)	0.0121(10)	1
O(8)	0.2727(3)	0.5046(3)	0.4006(2)	0.0139(11)	1
O(9)	0.1330(4)	0.3066(3)	0.3671(2)	0.0154(10)	1
O(10)	0.4399(4)	0.8483(3)	0.3688(2)	0.0143(10)	1
O(11)	0.3985(4)	0.6454(3)	0.3578(2)	0.0186(12)	1
O(12)	0.2098(4)	0.7692(3)	0.2731(2)	0.0160(11)	1
O(13)	0.4853(3)	0.7561(3)	0.21878(19)	0.0150(11)	1
O(14)	0.5002(4)	0.4827(3)	0.3561(2)	0.0148(11)	1
O(15)	0.8307(4)	0.4851(3)	0.2425(2)	0.0139(11)	1
O(16)	0.7349(3)	0.5547(3)	0.3840(2)	0.0133(10)	1
O(17)	0.6911(4)	0.3542(3)	0.3265(2)	0.0214(12)	1
O(18)	0.5844(3)	0.5291(3)	0.2133(2)	0.0124(10)	1
O(19)	0.6408(3)	0.6088(3)	-0.0012(2)	0.0122(9)	1
O(20)	0.4486(3)	0.5256(3)	0.08297(19)	0.0092(9)	1
O(21)	0.7646(4)	0.4876(3)	0.0992(2)	0.0127(10)	1
O(22)	0.6596(4)	0.6912(3)	0.1332(2)	0.0152(11)	1
O(23)	0.8654(4)	0.3435(3)	0.1522(2)	0.0192(12)	1
O(24)	0.9544(4)	0.1457(3)	0.1291(2)	0.0164(11)	1
O(25)	1.1019(4)	0.2603(4)	0.2273(2)	0.0201(12)	1
O(26)	0.8253(3)	0.2129(3)	0.2821(2)	0.0149(11)	1
O(27)	0.2675(12)	0.1643(8)	0.4941(6)	0.054(4)	0.549(19)
O(28)	0.5086(6)	0.1297(5)	-0.0092(3)	0.0350(19)	1
H(28a)	0.539(9)	0.117(8)	0.019(5)	0.04(2)	1
H(28b)	0.503(8)	0.095(7)	-0.044(5)	0.04(2)	1

^a H atoms were refined isotropically. All other atoms were refined anisotropically, except Cs(1) which was refined with third-order anharmonic tensor, and are given in the form of the isotropic equivalent displacement parameter U_{eq} defined by $U_{\text{eq}} = (1/3)\sum_{i=1}^3\sum_{j=1}^3 U_{ij}a_i^*a_j^*\bar{a}_i\bar{a}_j$.

Description of the Structure of $\text{Cs}_2\text{Ga}_6(\text{OH})_2(\text{PO}_4)_6 \cdot x\text{H}_2\text{O}$ ($x \approx 1.55$)

The projections of the structure of $\text{Cs}_2\text{Ga}_6(\text{OH})_2(\text{PO}_4)_6 \cdot x\text{H}_2\text{O}$ ($x \approx 1.55$) along [100] and [110] (Figures 1a and 2a, respectively) show that its three-dimensional framework is built from corner-sharing $\text{GaO}_4(\text{OH})$ bipyramids, GaO_4 tetrahedra, and PO_4 tetrahedra. The cesium cations and water molecules are located at the intersections of the tunnels running along the [100] and $\langle 110 \rangle$ directions. The $[\text{Ga}_6(\text{OH})_2(\text{PO}_4)_6]_{\infty}$ framework can easily be described from $[\text{Ga}_4(\text{OH})_2\text{P}_4\text{O}_{22}]_{\infty}$ layers parallel to (010) interconnected along [010] through tetrahedral $[\text{GaPO}_6]_{\infty}$ zigzag chains running along [100] (Figure 1a).

As shown in Figure 3a, the $[\text{GaPO}_6]_{\infty}$ chains simply consist of an alternation of corner-shared GaO_4 and PO_4 tetrahedra along [100]. Note that there are two independent $[\text{GaPO}_6]_{\infty}$ chains in the structure, formed by the Ga(3) and P(3) tetrahedra, on one hand, and by the Ga(6) and P(6)

tetrahedra on the other hand. In these chains, each PO_4 tetrahedron and each GaO_4 tetrahedron share two of their apexes with the $\text{GaO}_4(\text{OH})$ bipyramids and with the PO_4 tetrahedra of the $[\text{Ga}_4(\text{OH})_2\text{P}_4\text{O}_{22}]_{\infty}$ layers, respectively.

The resulting $[\text{Ga}_6(\text{OH})_2(\text{PO}_4)_6]_{\infty}$ three-dimensional framework forms six-sided tunnels running along *a*, delimited by the polyhedra of two $[\text{GaPO}_6]_{\infty}$ chains and of two $[\text{Ga}_4(\text{OH})_2\text{P}_4\text{O}_{22}]_{\infty}$ layers.

The projection of one $[\text{Ga}_4(\text{OH})_2\text{P}_4\text{O}_{22}]_{\infty}$ layer along [010] shows that it is built from $\text{GaO}_4(\text{OH})$ bipyramids and PO_4 tetrahedra, sharing their corners to form $[\text{Ga}_4(\text{OH})_2\text{P}_4\text{O}_{26}]_{\infty}$ waving ribbons parallel to *a* and assembled along *c* (Figure 4a). These ribbons can themselves be described as an assemblage of two independent $[\text{Ga}_2(\text{OH})_2\text{P}_2\text{O}_{12}]_{\infty}$ chains, in which the $\text{Ga}(\text{OH})\text{O}_4$ trigonal bipyramids alternate with the PO_4 tetrahedra. One of these chains corresponds to the sequence Ga(1)–P(2)–Ga(5)–P(4), whereas the other consists of Ga(2)–P(1)–Ga(4)–P(5). The connection between the two $[\text{Ga}_2(\text{OH})_2\text{P}_2\text{O}_{12}]_{\infty}$ chains to form a $[\text{Ga}_4(\text{OH})_2\text{P}_4\text{O}_{26}]_{\infty}$ waving ribbon is made in the following way: each Ga(1) and Ga(4) bipyramids share one apex with P(1) and P(4), respectively, and one apex with Ga(2) and Ga(5), respectively. Note that the OH groups are shared between the gallium polyhedra, i.e., between Ga(1) and Ga(2) and between Ga(4) and Ga(5). Thus, each $[\text{Ga}_4(\text{OH})_2\text{P}_4\text{O}_{22}]_{\infty}$ layer results from the junction of $[\text{Ga}_4(\text{OH})_2\text{P}_4\text{O}_{26}]_{\infty}$ waving ribbons along *c*, the P(2) and P(5) tetrahedra of one ribbon sharing one apex with the Ga(5) and Ga(2) trigonal bipyramids of the next ribbon, respectively. This assemblage leads to the presence in the layers of two types of windows: small rectangular ones and large octagonal ones (Figure 4a). In the three-dimensional $[\text{Ga}_6(\text{OH})_2(\text{PO}_4)_6]_{\infty}$ framework, two successive layers (linked through the $[\text{GaPO}_6]_{\infty}$ zigzag chains), are related through the 2_1 axis parallel to *b* ($1/4, y, 0$), so that the large octagonal windows are not superimposed along *b* but along the $\langle 110 \rangle$ directions, to form eight-sided tunnels (Figure 2a). The cesium cations and water molecules are located at the intersection of these tunnels with the six-sided tunnels parallel to *a* (Figure 1a).

This novel structure exhibits close relationships with that of the phosphates $(\text{CH}_3\text{NH}_3)_2\text{M}_6(\text{OH})_2(\text{PO}_4)_6$.^{14,15} The 3D-frameworks are in fact very similar but with different distortions. Nevertheless, it exhibits a different symmetry, monoclinic instead of orthorhombic, and a different location of the Cs^+ cations and H_2O molecules compared to that of the $(\text{CH}_3\text{NH}_3)^+$ cations. These features suggest the possible existence of the nonhydrated form “ $\text{Cs}_2\text{Ga}_6(\text{OH})_2(\text{PO}_4)_6$ ”. We have thus studied the dehydration of this novel gallophosphate.

Topotactic Dehydration of $\text{Cs}_2\text{Ga}_6(\text{OH})_2(\text{PO}_4)_6 \cdot x\text{H}_2\text{O}$ ($x \approx 1.55$): Transmission Electron Microscopy and X-ray Powder Diffraction Studies

The transmission electron microscopy investigation was carried out in order to check the formation of nano-twinning domains, commonly observed in pseudo-orthorhombic structures. However, the first experiments evidenced that the sample was sensitive to the electron beam irradiation.

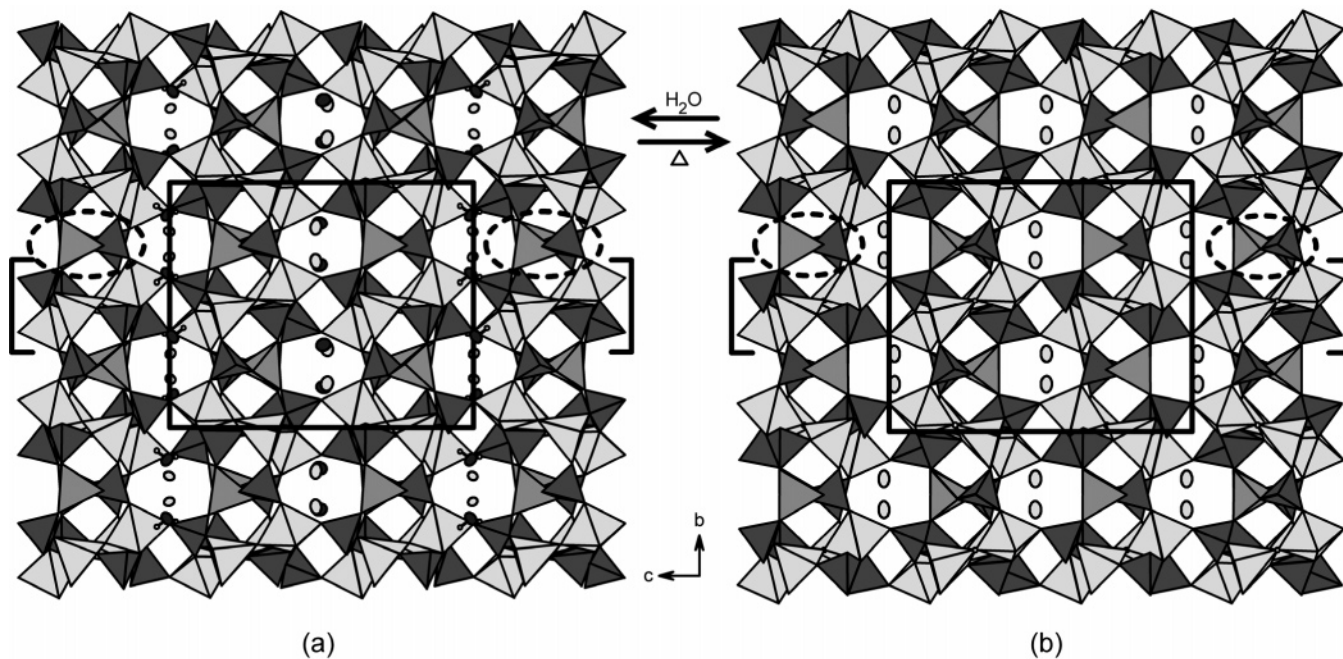


Figure 1. Projections along [100] of the structures of $\text{Cs}_2\text{Ga}_6(\text{OH})_2(\text{PO}_4)_6 \cdot x\text{H}_2\text{O}$ ($x \approx 1.55$) (a) and its dehydrated form $\text{Cs}_2\text{Ga}_6(\text{OH})_2(\text{PO}_4)_6$ (b). For each structure, one $[\text{Ga}_4(\text{OH})_2\text{P}_4\text{O}_{22}]_\infty$ layer is placed into brackets and two $[\text{GaPO}_6]_\infty$ chains are circled with bold dotted lines. PO_4 tetrahedra are colored in dark gray, GaO_4 tetrahedra in medium gray, and $\text{GaO}_4(\text{OH})$ trigonal bipyramids in light gray. Cesium cations are drawn with light gray circles and water molecules with black circles (displacement ellipsoid of cesium and oxygen atoms at 70% probability level). Small isotropic circles represent hydrogen atoms. For the hydrated compound (a), Cs(1) and H_2O (27) are located in the cell at $z = 1/2$ and Cs(2) and H_2O (28) at $z = 0$.

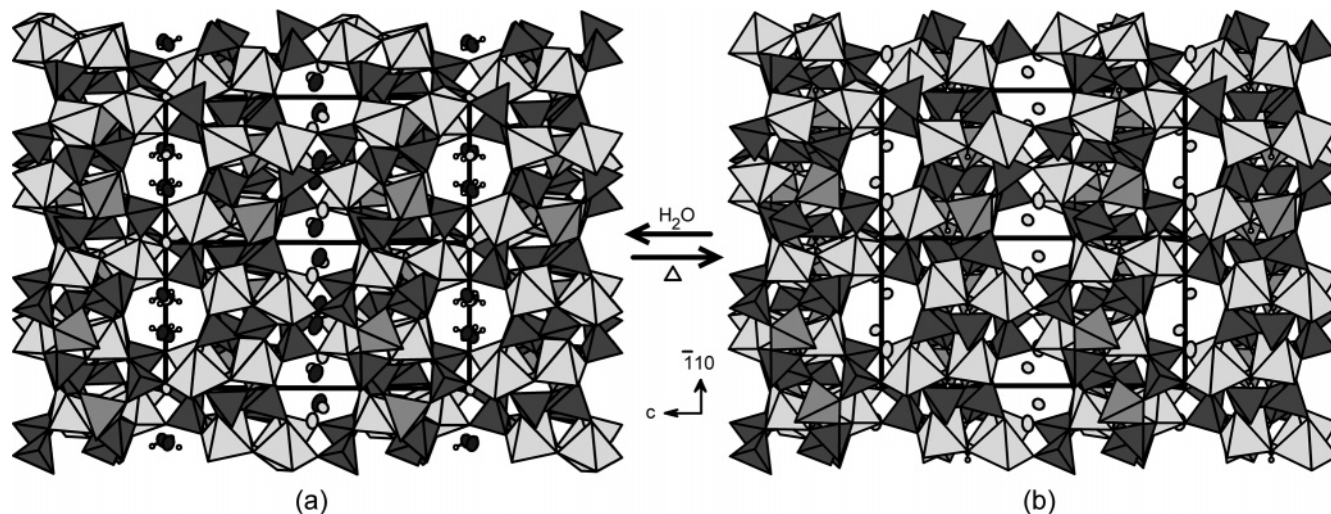


Figure 2. Projections along [110] of the structures of $\text{Cs}_2\text{Ga}_6(\text{OH})_2(\text{PO}_4)_6 \cdot x\text{H}_2\text{O}$ ($x \approx 1.55$) (a) and $\text{Cs}_2\text{Ga}_6(\text{OH})_2(\text{PO}_4)_6$ (b). See Figure 1 for complete legend.

A first series of observations was therefore carried out using a low beam intensity, to avoid any transformation by the beam irradiation. In these conditions, the reconstruction of the reciprocal space by tilting around the crystallographic axes leads to a monoclinic cell with $a \approx 10.2 \text{ \AA}$, $b \approx 13.9 \text{ \AA}$, $c \approx 17.3 \text{ \AA}$, and β slightly different but very close to 90° . The conditions limiting the reflections are $h0l$: $h = 2n$ and $0k0$: $k = 2n$, consistent with the $P2_1/a$ space group. The $[001]$ and $[010]$ ED patterns are given in Figures 5a and 5b, respectively; the $0k0 = 2n + 1$ reflections in Figure 5a (see small white arrows) result from double diffraction phenomena, as checked by tilting around \bar{b}^* . The sharpness of the reflections attests to the high crystallinity of the grains. The bright and dark field imaging techniques confirm this quality of the sample and show that the width of the twinning

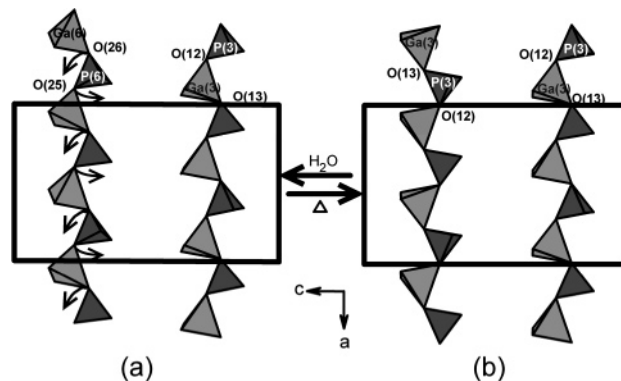


Figure 3. View along [010] of the $[\text{GaPO}_6]_\infty$ zigzag chains parallel to a in $\text{Cs}_2\text{Ga}_6(\text{OH})_2(\text{PO}_4)_6 \cdot x\text{H}_2\text{O}$ ($x \approx 1.55$) (a) and in $\text{Cs}_2\text{Ga}_6(\text{OH})_2(\text{PO}_4)_6$ (b). The arrows indicate in which way some of the oxygen atoms are shifted during the topotactic dehydration. See Figure 1 for complete legend.

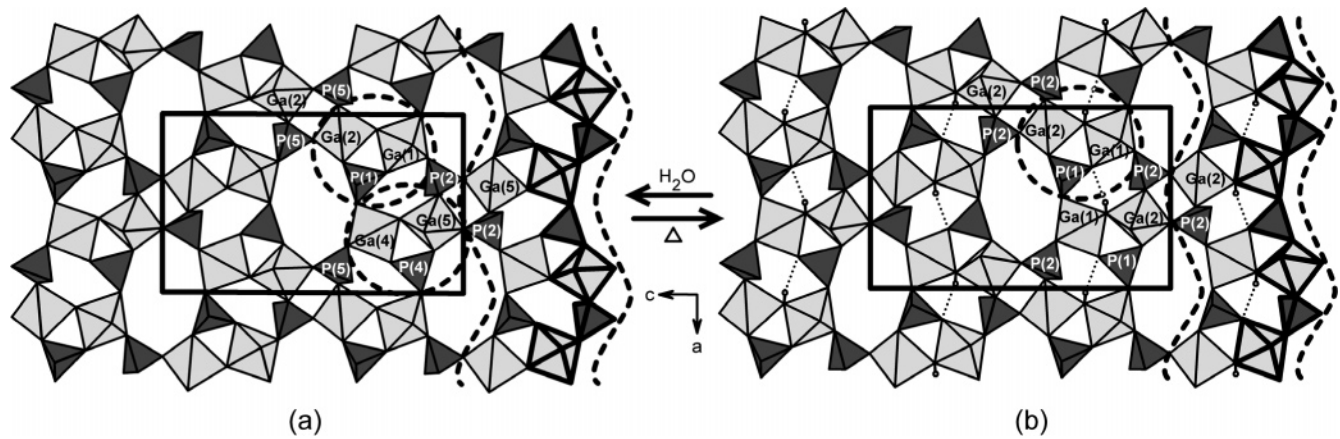


Figure 4. Projections along $[010]$ of one $[\text{Ga}_4(\text{OH})_2\text{P}_4\text{O}_{22}]_\infty$ layer parallel to (010) in $\text{Cs}_2\text{Ga}_6(\text{OH})_2(\text{PO}_4)_6 \cdot x\text{H}_2\text{O}$ ($x \approx 1.55$) (a) and $\text{Cs}_2\text{Ga}_6(\text{OH})_2(\text{PO}_4)_6$ (b). $\text{Ga}_2(\text{OH})\text{PO}_{10}$ units are circled with bold dotted lines. Polyhedra of one $[\text{Ga}_2(\text{OH})_2\text{P}_2\text{O}_{12}]_\infty$ undulating chain are stressed with bold lines and one $[\text{Ga}_4(\text{OH})_2\text{P}_4\text{O}_{26}]_\infty$ waving ribbon is wrapped in a bold dotted line. Hydrogen bonding in the dehydrated compound (b) is evidenced with thin dotted lines. For other legends see Figure 1.

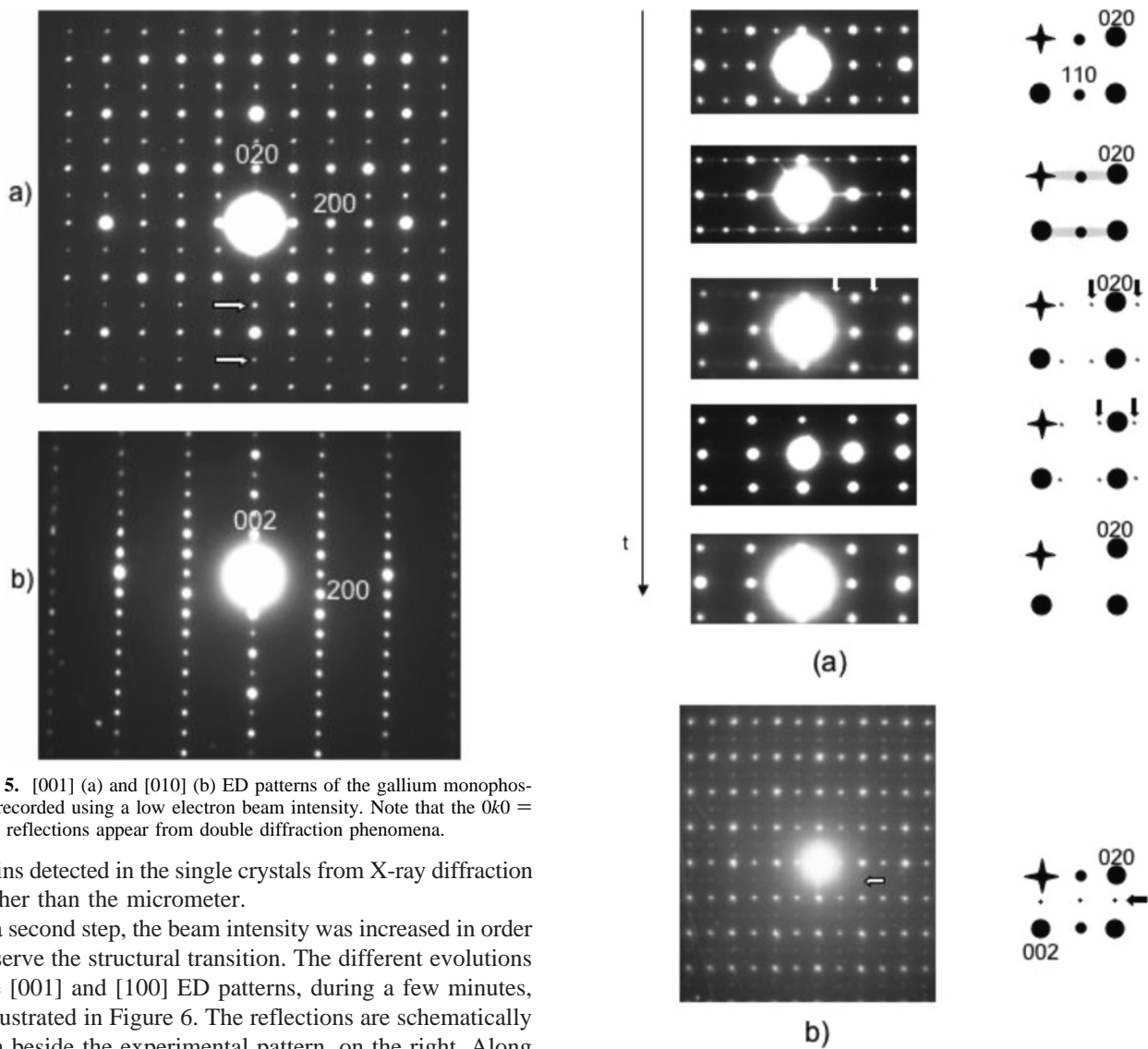


Figure 5. $[001]$ (a) and $[010]$ (b) ED patterns of the gallium monophosphate, recorded using a low electron beam intensity. Note that the $0k0 = 2n + 1$ reflections appear from double diffraction phenomena.

domains detected in the single crystals from X-ray diffraction is higher than the micrometer.

In a second step, the beam intensity was increased in order to observe the structural transition. The different evolutions of the $[001]$ and $[100]$ ED patterns, during a few minutes, are illustrated in Figure 6. The reflections are schematically drawn beside the experimental pattern, on the right. Along $[001]$, the structural transitions occur by steps (Figure 6a): the first image is that of the monoclinic phase ($hk0$: no condition except that $(h00 = 2n + 1)$ and $(0k0 = 2n + 1)$ are generated by double diffraction phenomena). In the second one, the monoclinic subcell is retained but streaky lines appear along \bar{b}^* , attesting to disorder phenomena along

Figure 6. Evolution with time of the $[001]$ (a) and $[100]$ (b) ED patterns, increasing the electron beam intensity.

that direction. In the third one, the $hk0$ reflections with $k = 2n + 1$ are no longer observed, indicating a symmetry change, but extra weak reflections (indicated by small arrows) in incommensurate positions are observed (in the

present example, $\vec{q}^* \approx 0.6\vec{b}^*$). The positions of the satellites vary ($\vec{q}^* \approx 0.5\vec{b}^*$) and their intensity decreases with the irradiation time, as shown in the fourth image. Last, in the [100] ED patterns, one observes the condition $hk0: k = 2n$. Along [100], the positions of the reflections do not change, one only observes the decrease of the intensity of the reflections $0kl$, $l = 2n + 1$, as shown in Figure 6b where they are scarcely visible (see small arrow), up to the complete extinction. The [010] ED patterns remain unchanged during the transition. At the end of the evolution, the cell is orthorhombic, with parameters close to the initial ones, and the conditions limiting the reflections are as follows: $hk0: k = 2n$; $0kl$, $l = 2n$, and $h0l: h = 2n$, compatible with the space group $Pcab$. These results definitely demonstrate that the dehydration is topotactic.

The transition is not reversible in situ, in agreement with the thermogravimetric analyses which correlate it with water molecules loss. The interesting point of this transition is viewed along [001] since it clearly demonstrates that the transition is not of the first order but is stabilized by the pinning of local order-disorder phenomena, in incommensurate modulated microstructures, the amplitude of the modulation vector being ($\vec{q}^* \approx v\vec{b}^*$). This effect suggests that the topotactic reaction takes place layer by layer by groups of (010) layers.

Taking into consideration the results of thermogravimetric analysis and TEM studies, X-ray powder diffraction was carried out versus temperature, using a Philips X-Pert Pro diffractometer, for the Cu K α radiation, equipped with a Paar Physica TCU100 temperature control unit. The XRPD pattern registered at room temperature leads to cell parameters (refined with the program FullProf²⁰), very similar to those obtained from the single-crystal study for $\text{Cs}_2\text{Ga}_6(\text{OH})_2(\text{PO}_4)_6 \cdot 1.55\text{H}_2\text{O}$, $a = 10.2220(6)$ Å, $b = 13.9565(7)$ Å, $c = 17.2629(8)$ Å, and $\beta = 90.452(2)^\circ$. This result confirms the monoclinic symmetry, with a more reliable value of the β angle, since the twinning does not affect the XRPD pattern. At 100 °C, no modification of the pattern is observed, confirming that the weight loss in TGA is only due to physisorbed water, whereas between 160 and 225 °C a mixture of two closely related phases, with respective monoclinic and orthorhombic symmetries, is observed. Finally at 350 °C, the peaks of the monoclinic phase $\text{Cs}_2\text{Ga}_6(\text{OH})_2(\text{PO}_4)_6 \cdot 1.55\text{H}_2\text{O}$ have completely disappeared, and all the peaks were indexed in an orthorhombic cell, space group $Pcab$, with $a = 10.2278(7)$ Å, $b = 13.944(1)$ Å, and $c = 17.105(1)$ Å. The latter phase, $\text{Cs}_2\text{Ga}_6(\text{OH})_2(\text{PO}_4)_6$, is stable in a dry atmosphere at room temperature: its refined cell parameters are then, as expected, slightly smaller: $a = 10.1694(6)$ Å, $b = 13.9850(8)$ Å, and $c = 16.952(1)$ Å.

The detailed results of XRPD patterns refinements are given as Supporting Information (S3).

These results, together with the TGA and TEM studies, suggest strongly that $\text{Cs}_2\text{Ga}_6(\text{OH})_2(\text{PO}_4)_6 \cdot 1.55\text{H}_2\text{O}$ is dehydrated topotactically into $\text{Cs}_2\text{Ga}_6(\text{OH})_2(\text{PO}_4)_6$, whose struc-

ture should still be more closely related to that of $(\text{CH}_3\text{NH}_3)_2\text{M}_6(\text{OH})_2(\text{PO}_4)_6$.^{14,15}

The reaction is reversible, but is slow compared to normal zeolitic compounds. Exposure to air humidity is not sufficient to recover the hydrated phase $\text{Cs}_2\text{Ga}_6(\text{OH})_2(\text{PO}_4)_6 \cdot 1.55\text{H}_2\text{O}$. In contrast, a single crystal of the dehydrated phase $\text{Cs}_2\text{Ga}_6(\text{OH})_2(\text{PO}_4)_6$ with orthorhombic symmetry is completely transformed into the hydrated one $\text{Cs}_2\text{Ga}_6(\text{OH})_2(\text{PO}_4)_6 \cdot x\text{H}_2\text{O}$ with monoclinic symmetry when placed for 2 h in suspension in water.

Structure Determination and Description of $\text{Cs}_2\text{Ga}_6(\text{OH})_2(\text{PO}_4)_6$

To obtain the dehydrated phase, crystals of $\text{Cs}_2\text{Ga}_6(\text{OH})_2(\text{PO}_4)_6 \cdot x\text{H}_2\text{O}$ were heated at 350 °C for about 16 h in a platinum crucible. Single crystals of the resulting non-hydrated phase were then selected for the structure determination.

The single crystal used for the structure determination of $\text{Cs}_2\text{Ga}_6(\text{OH})_2(\text{PO}_4)_6$ presents a stick-like morphology, with dimensions of $0.337 \times 0.063 \times 0.046$ mm³. Its X-ray diffraction data were collected with the parameters given in Table 1. Large diffraction spots were observed, due to a high mosaicity. Intensities were integrated considering an isotropic mosaicity. A monoclinic symmetry was no longer observed, but instead, a strict orthorhombic cell, with parameters close to those of the hydrated phase (Table 1), in agreement with the XRPD studies.

The systematic absences $0kl: l = 2n + 1$, $h0l: h = 2n + 1$, and $hk0: k = 2n + 1$ observed for this phase correspond to the centrosymmetric space group $Pcab$ (No. 61), in agreement with the TEM observations. The structure was refined similarly to the hydrated phase, with anisotropic displacement parameters for all the atoms, leading to $R = 0.0363$ and $R_w = 0.0380$. However, the presence of two quite strong electronic density residues of 4.21 and 2.42 e⁻/Å³ around Cs(1) incited us to refine the thermal displacement parameters of this atom using a third-order anharmonic tensor. There were no more strong residues around Cs(1) after this refinement (maximal residue of 0.87 e⁻/Å³) and significant lower values of the reliability factors were obtained ($R = 0.0274$ and $R_w = 0.0279$).

The BVS calculations confirmed that, as in the monoclinic compound, there is an hydroxyl group on the oxygen atom bonding the two gallium trigonal bipyramids (O(5)). The BVS calculations for all other atoms lead to the expected values. The examination of the electronic residues observed on the Fourier difference map allowed us to determine the position of the hydrogen atom of the hydroxyl group. Its atomic parameters were refined (isotropic displacement parameter). The final reliable factors are $R = 0.0272$ and $R_w = 0.0274$. The corresponding atomic coordinates, equivalent isotropic thermal parameters, and their estimated standard deviations are listed in Table 3. The distances and angles in the structure, as well as the BVS calculations, are given in the Supporting Information (S1b and S2b).

The phase $\text{Cs}_2\text{Ga}_6(\text{OH})_2(\text{PO}_4)_6$ is isotopic with $(\text{CH}_3\text{NH}_3)_2\text{Ga}_6(\text{OH})_2(\text{PO}_4)_6$.¹⁴ The projections of the structure of this dehydrated hydroxyphosphate along [100] and [110] (Figures

(20) Rodriguez-Carvajal J. FULLPROF: A Program for Rietveld Refinement and Pattern Matching Analysis; Abstracts of the Satellite Meeting on Powder Diffraction of the XV Congress of the IUCr, Toulouse, France, 1990; p 127.

Table 3. Positional Parameters, Atomic Displacement Parameters, and Their Estimated Standard Deviations in $\text{Cs}_2\text{Ga}_6(\text{OH})_2(\text{PO}_4)_6$ ^a

atom	x	y	z	U_{eq} (\AA^2)
Cs(1)	0.43435(4)	0.31088(4)	0.48204(3)	0.03661(6)
Ga(1)	0.16503(2)	0.520252(15)	0.195690(13)	0.00788(4)
Ga(2)	0.12180(2)	0.437821(15)	0.395918(13)	0.00733(4)
Ga(3)	0.39086(2)	0.756615(15)	0.302555(13)	0.00881(5)
P(1)	0.37269(5)	0.54354(4)	0.34592(3)	0.00857(10)
P(2)	0.37488(5)	0.42836(3)	0.08422(3)	0.00701(9)
P(3)	0.14368(5)	0.74471(3)	0.19854(3)	0.00771(9)
O(1)	-0.00499(14)	0.51620(11)	0.13887(10)	0.0136(3)
O(2)	0.32867(15)	0.53161(13)	0.26034(9)	0.0151(4)
O(3)	0.23736(14)	0.44411(11)	0.11804(9)	0.0123(3)
O(4)	0.18214(17)	0.64725(10)	0.16651(10)	0.0153(4)
O(5)	0.08546(15)	0.47128(12)	0.28562(9)	0.0126(3)
O(6)	0.13841(15)	0.38661(11)	0.50204(9)	0.0118(3)
O(7)	-0.04925(14)	0.47719(10)	0.41702(9)	0.0104(3)
O(8)	0.26627(14)	0.51591(11)	0.40581(9)	0.0131(3)
O(9)	0.17593(17)	0.31504(11)	0.36692(10)	0.0162(4)
O(10)	0.44881(15)	0.85438(11)	0.36393(10)	0.0133(3)
O(11)	0.40718(17)	0.64993(11)	0.36283(11)	0.0175(4)
O(12)	0.21810(15)	0.76830(13)	0.27486(10)	0.0158(4)
O(13)	0.49506(15)	0.75100(13)	0.21553(10)	0.0153(4)
H(5)	0.025(4)	0.474(3)	0.283(3)	0.038(12)

^a H(5) atoms were refined isotropically. All other atoms were refined anisotropically, except Cs(1) which was refined with third-order anharmonic tensor, and are given in the form of the isotropic equivalent displacement parameter U_{eq} defined by $U_{\text{eq}} = \langle \frac{1}{3} \sum_{i=1}^3 \sum_{j=1}^3 U_{ij} a_i^* a_j^* \bar{a}_i \bar{a}_j \rangle$.

1b and 2b) show its great similarity with the hydrated one (Figures 1a and 2a): one indeed observes a similar $[\text{Ga}_6(\text{OH})_2(\text{PO}_4)_6]_{\infty}$ framework forming six-sided and eight-sided intersecting tunnels running along a and $\langle 110 \rangle$, respectively. Remarkably, the $[\text{Ga}_4(\text{OH})_2\text{P}_4\text{O}_{22}]_{\infty}$ layers (Figure 4) exhibit the same symmetry in the hydrated phase (Figure 4a) and in the nonhydrated phase (Figure 4b), characteristic of the $Pcab$ orthorhombic space group. The two structures differ in fact by the geometry of the tetrahedral $[\text{GaPO}_6]_{\infty}$ chains: one indeed observes identical chains compatible with $Pcab$ in the dehydrated phase (Figure 3b), whereas two different kinds of chains, implying the $P2_1/a$ space group, are observed in the hydrated phase (Figure 3a). In fact, this different symmetry of the two structures originates mainly from the position of the Cs^+ cations as shown from the projections along b (Figure 7): the departure of water in the hydrated phase is indeed accompanied by a displacement of Cs(2) by about 3 \AA in the tunnels along a , so that its new position in the dehydrated phase (Figure 7b) has become close to that of the H_2O molecules in the hydrated phase (Figure 7a). In

this respect, the dehydrated phase is similar to $(\text{CH}_3\text{NH}_3)_2\text{Ga}_6(\text{OH})_2(\text{PO}_4)_6$, the positions of the Cs^+ cations being close to those of the methylammonium cations.

The geometry of the polyhedra is very similar in the two structures, with P–O bonds ranging from about 1.51 to 1.55 \AA , the longest P–O distance corresponding to the oxygen atoms shared with a GaO_4 tetrahedron. The regular geometry of the PO_4 tetrahedra is confirmed by the O–P–O angles comprised between 104° and 113° . The geometry of the GaO_4 tetrahedra is that usually observed, with Ga–O distances ranging from 1.807 to 1.831 \AA . Note that, in the hydrated phase, the Ga(6) tetrahedron is slightly more distorted than the Ga(3) one, due to the absence of $Pcab$ symmetry between two independent $[\text{GaPO}_6]_{\infty}$ chains. The $\text{Ga}_4(\text{OH})$ bipyramids adopt very similar geometries in both structures with three equatorial distances ranging from 1.837 to 1.885 \AA and two longer apical bonds ranging from 1.933 to 1.998 \AA . Note that the Ga(1) and Ga(4) bipyramids are the most distorted. It must also be noticed that the hydroxyl groups correspond to the O(5) and O(18) in the hydrated phase and to O(5) in the dehydrated one. Moreover, the atomic coordinates of the hydrogen atom could be determined in the dehydrated phase, forming a O–H bond of 0.62 \AA and a hydrogen bond with O(2) of 2.12 \AA .

The Cs^+ cations exhibit a 9-fold and a 10-fold coordination in the hydrated and dehydrated phases, respectively. In the hydrated phase, the Cs(1) cation exhibits significantly shorter Cs–O distances (down to 2.90 \AA) than the Cs(2) cation (down to 3.08 \AA), whereas the Cs–O distances in the dehydrated phase (down to 3.12 \AA) are intermediate between those observed for Cs(1) and Cs(2) in the hydrated phase.

The detailed angles and distances for both studied compounds are given as Supporting Information (S1).

Conclusions

The investigation of the Cs–Ga–P–O system, using hydrothermal synthesis, shows the possibility of generating a new type of intersecting tunnel structure, $\text{Cs}_2\text{Ga}_6(\text{OH})_2(\text{PO}_4)_6 \cdot 1.55\text{H}_2\text{O}$, by introducing simultaneously water beside Cs^+ cation in the structure. The latter structure is closely related to that of the methylammonium phases $(\text{CH}_3\text{NH}_3)_2\text{M}_6(\text{OH})_2(\text{PO}_4)_6$ ($\text{M} = \text{Ga}, \text{Al}$)^{14–15} and differs from the latter

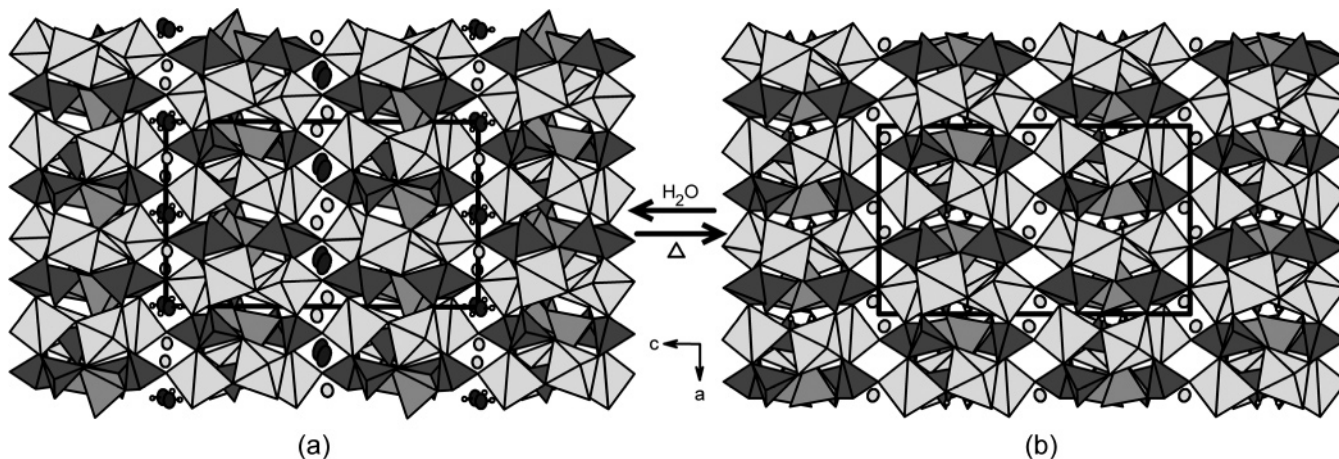


Figure 7. Projections along $[010]$ of the structures of $\text{Cs}_2\text{Ga}_6(\text{OH})_2(\text{PO}_4)_6 \cdot x\text{H}_2\text{O}$ ($x \approx 1.55$) (a) and $\text{Cs}_2\text{Ga}_6(\text{OH})_2(\text{PO}_4)_6$ (b), evidencing the mobility of Cs(2) cation ($z = 0$) in the tunnel along a during the topotactic dehydration. See Figure 1 for complete legend.

by its monoclinic symmetry, due to the different configurations of the $[\text{GaPO}_6]_\infty$ chains and the different positions of the Cs^+ and H_2O species with respect to the methylammonium cations. A topotactic dehydration reaction, leading to the phosphate $\text{Cs}_2\text{Ga}_6(\text{OH})_2(\text{PO}_4)_6$, with a different orthorhombic symmetry, and isotopic to $(\text{CH}_3\text{NH}_3)_2\text{M}_6(\text{OH})_2(\text{PO}_4)_6$ ($\text{M} = \text{Ga}, \text{Al}$), is observed for the first time in this structural family. Remarkably, the cesium cation exhibits an unusual mobility during the topotactic dehydration, moving between two sites separated by a distance of about 3 Å. It is also shown from the TEM observations that cesium may occupy several positions successively during the dehydration, so that this reaction can be considered as a soft second-order reaction. The reversibility of the reaction in the presence of water, which changes back the geometry of the $[\text{GaPO}_6]_\infty$ chains, shows the extraordinary flexibility of the $[\text{Ga}_6(\text{OH})_2(\text{PO}_4)_6]_\infty$ framework, which is moreover stable up to 350 °C.

These results also suggest that the possibility of creating frameworks susceptible to hosting simultaneously cesium cations and larger organic cations or molecules should be considered.

Acknowledgment. We thank Dr. O. Pérez for helpful discussion. The authors gratefully acknowledge the Région Basse-Normandie, the Ministère de la Recherche, and the European Union (network of excellence FAME) for financial support.

Supporting Information Available: Tables of angles and distances in the two studied compounds; tables of the BVS calculations for the two studied compounds; table giving the XRPD refinement results versus temperature; X-ray crystallographic information file (CIF) for both studied compounds. This material is available free of charge via the Internet at <http://pubs.acs.org>.

CM060275Z